iScience

CellPress
OPEN ACCESS

Article

Nuclear *NME1* enhances the malignant behavior of A549 cells and impacts lung adenocarcinoma patient prognosis

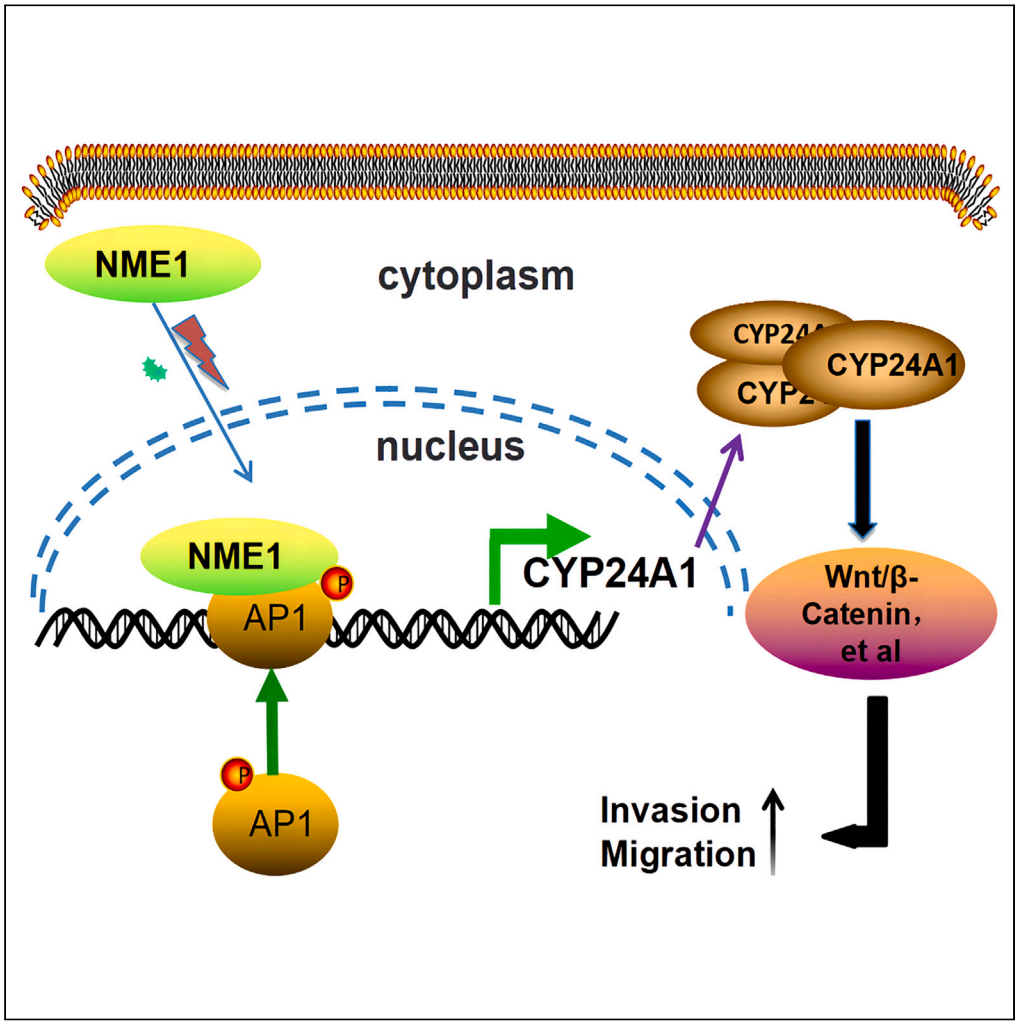

Mingfang Xu, Yingda Liu, Xunjie Kuang, ..., Xiaodong Zhao, Xueqin Yang, Mengxia Li

xusiyi023@126.com (M.X.)
yangxueqin@hotmail.com (X.Y.)
mengxia.li@outlook.com (M.L.)

Highlights

NME1 is both a promoter and inhibitor of cancer metastasis

The dual role of *NME1* in tumors is related to nuclear and cytoplasmic localization

Nuclear NME1 up-regulates *CYP24A1* expression in A549 cells

The binding of *NME1* and JUN promotes the transcriptional activity of JUN

Xu et al., iScience *27*, 110286
July 19, 2024
https://doi.org/10.1016/j.isci.2024.110286

iScience

CellPress
OPEN ACCESS

Article

Nuclear *NME1* enhances the malignant behavior of A549 cells and impacts lung adenocarcinoma patient prognosis

Mingfang Xu,[1,2,3,4,*] Yingda Liu,[1,3] Xunjie Kuang,[1] Yu Pu,[1] Yuzhu Jiang,[1] Xiaodong Zhao,[2] Xueqin Yang,[1,*] and Mengxia Li[1,*]

SUMMARY

***NME1* is a metastatic suppressor inconsistently reported to have multiple roles as both a promoter and inhibitor of cancer metastasis. Nevertheless, the specific mechanism behind these results is still unclear. We observed that A549 cells with stable transfer of *NME1* into the nucleus (A549-nNm23-H1) exhibited significantly increased migration and invasion activity compared to vector control cells, which was further enhanced by over-expressing CYP24A1 ($p < 0.001$). *NME1* demonstrated the ability to safely attach to and amplify the transcription activation of JUN, consequently leading to the up-regulation of *CYP24A1*. Analysis of clinical data showed a positive relationship between nuclear *NME1* levels and *CYP24A1* expression. Furthermore, they were positively associated with postoperative distant metastasis and negatively correlated with prognosis in those with early stage lung adenocarcinoma. In conclusion, the data presented provides a new understanding of the probable pathways by which nuclear *NME1* facilitates tumor metastasis, establishing the groundwork for future prediction and treatment of tumor metastasis.**

INTRODUCTION

The 5-year survival rates for lung cancer patients diagnosed between 2010 and 2014 varied between 10% and 20% in most countries.[1] The leading cause of mortality among lung cancer patients was the spread of cancer to other parts of the body. There is a pressing requirement for developing novel biomarkers and targets for therapeutic intervention that can extend patient survival and enhance the overall quality of life among lung cancer patients who have undergone surgery.

NME1, also called Nm23-H1 or nucleoside diphosphate kinase A (*NDPK-A*), was first identified as a gene suppressing metastasis in human cells in 1988.[2] *NME1* primarily localizes to the cytoplasmic, although it sometimes *trans*-locates into the nucleus. Nuclear translocation of *NME1* can occur in response to factors such as irradiation or viral infection, and it can counteract the anti-metastatic role that this protein otherwise plays.[3,4] *NME1* has been observed to play diverse roles in different cellular contexts. These roles include its capacity to regulate gene expression, transmit signals inside cells, control cellular growth and specialization, maintain the balance of nucleotides within cells, and facilitate the internalization of G protein-coupled receptors. These mechanisms can shape tumor cell proliferative, migratory, invasive, and apoptotic activity. *NME1* down-regulation has been demonstrated to be closely associated with invasive transitions in the context of cancer progression[5] and inhibiting *NME1* can contribute to the metastasis of breast tumors in mice.[6] Exosomal or liposomal *NME1* can suppress breast cancer cell migration and motility.[7] In light of these impacts, researchers have attempted to increase the expression of *NME1* to re-establish its anti-metastatic function within the framework of metastatic cancer.[8] One meta-analysis of 25 studies determined a negative association between *NME1* expression and both TNM stage and lymph node status, with these levels negatively correlated with rates of both 3- and 5-year survival.[9] Increased levels of *NME1* gene expression are expected to improve prognostic outcomes in individuals diagnosed with lung cancer. Surprisingly, several studies document high levels of *NME1* expression in the later stages of the disease,[10–13] with nuclear *NME1* promoting metastatic progression and early recurrence in various cancers.[14,15]

Previous work from our group also revealed that patients exhibiting nuclear *NME1* expression in excised lung tumor samples faced a greater risk of early recurrence or distant metastasis,[16] suggesting that in addition to suppressing metastasis, *NME1* may promote tumor cell invasion and metastatic progression in specific contexts. *NME1* has a dual role in promoting and inhibiting the spread of tumor cells. Although the role of nuclear localization of *NME1* in promoting metastasis is well established, the specific mechanisms responsible for this effect have yet to be elucidated.

[1]Department of Cancer Center, Daping Hospital, Army Medical University, Chongqing, China
[2]The Second Affiliated Hospital of Chongqing Medical University, Chongqing, China
[3]These authors contributed equally
[4]Lead contact
*Correspondence: xusiyi023@126.com (M.X.), yangxueqin@hotmail.com (X.Y.), mengxia.li@outlook.com (M.L.)
https://doi.org/10.1016/j.isci.2024.110286

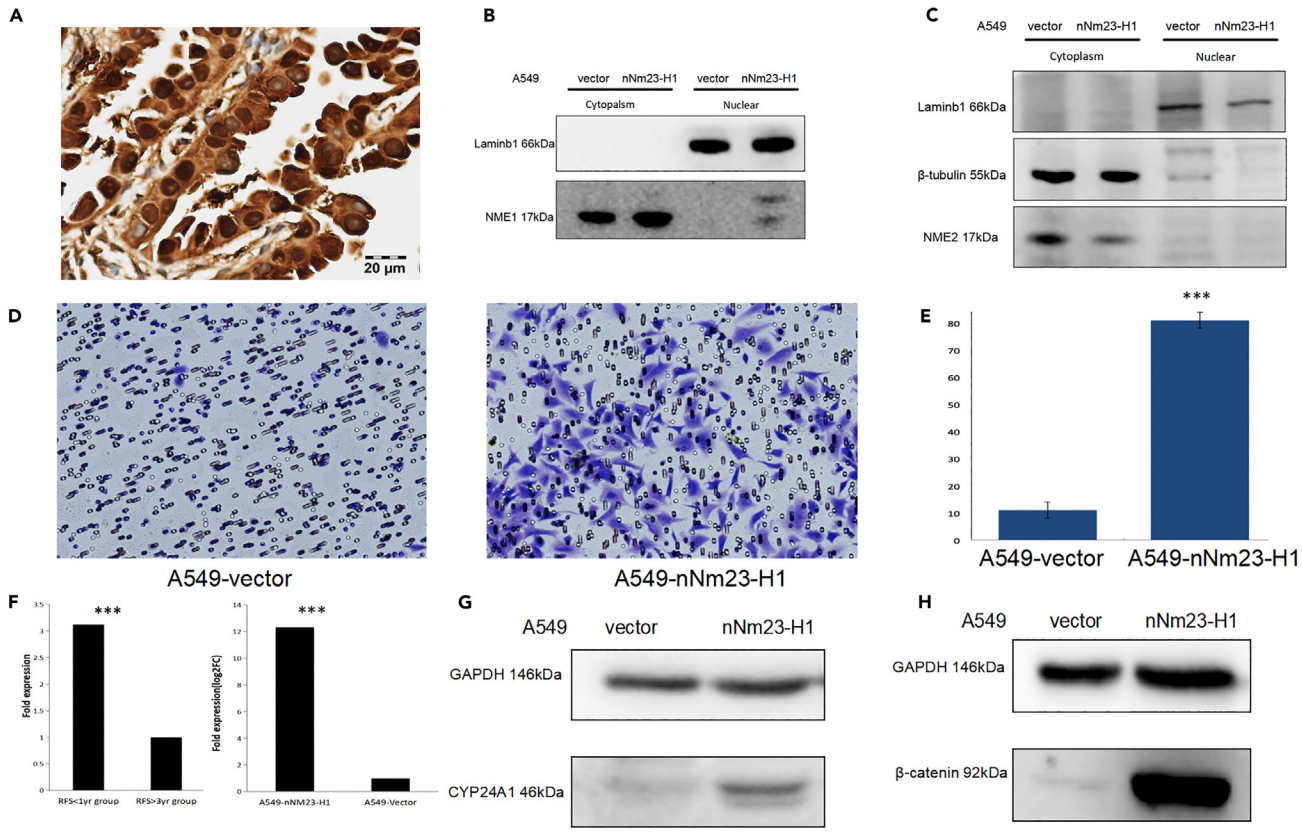

Figure 1. Patients with early postoperative metastasis of lung cancer are prone to nuclear expression of NME1 in lung cancer cells, and NME1 nuclear translocation enhances the migration ability of A549 cells

(A) Immunohistochemical expression of NME1 in the nucleus of lung cancer.

(B and C)The expression of NME1 and NME2 in the cytoplasm and nucleus was confirmed in A549-vector and A549-nNm23-H1 cells using western blotting.

(D and E) NME1 nuclear translocation enhances the migration ability of A549 cells. Data are the means ± SEM of three experiments. ***$p < 0.001$.

(F) CYP24A1 is highly expressed in A549-nNm23-H1 cells and in patients with early postoperative metastasis of lung cancer. Data are the means ± SEM of three experiments. ***$p < 0.001$.

(G and H) NME1 nuclear translocation up-regulates CYP24A1 and its downstream pathways expression of β-catenin protein.

The current study primarily examines A549 cells and employs advanced techniques such as super-shift electrophoretic mobility shift assay (EMSA) and dual-luciferase reporter assay to explore how nuclear *NME1* promotes tumor metastasis.

RESULTS

Nuclear *NME1* promotes A549 cell malignancy

Initially, we evaluated the biological attributes of A549 cells by examining the nuclear translocation of *NME1*. In order to achieve this objective, we used A549 cells that had undergone *NME1* nuclear translocation (A549-nNm23-H1), *NME1* knockdown (A549-shNm23-H1), and vector control cells (Figures 1B, S1A, and S1B). We also verified that NME2 did not undergo nuclear translocation in A549-nNm23-H1 (Figure 1C). We have confirmed and reported in our previous studies that NLS-Nm23-H1 does not affect the distribution of endogenous *NME1*.[16] Relative to the A549-vector cells, *NME1* nuclear translocation significantly enhanced A549 cell migratory activity in transwell migration assays (Figures 1D and 1E).

Nuclear *NME1* promotes *CYP24A1* over-expression in A549 cells

The mechanistic drivers of the phenotypic variations associated with *NME1* nuclear localization were assessed using an RNA sequencing approach. The transcriptomic profiles of the A549-nNm23-H1 and A549-siNm23-H1 cells were compared to the A549-vector cells, with three biological replicates per treatment group. In total, 144 up-regulated and 113 down-regulated genes were found to be significantly differentially expressed due to the nuclear translocation of *NME1* (FDR ≤0.01, log2 FC ≥ 10). RNA-seq analyses of lung adenocarcinoma samples that had rapidly metastasized within 1-year post-surgery (recurrence-free survival [RFS] < 1 year) and those that did not recur within 3 years of follow-up (RFS >3 years) from our hospital, revealing a total of 734 differentially expressed genes (log2 FC ≥ 2).

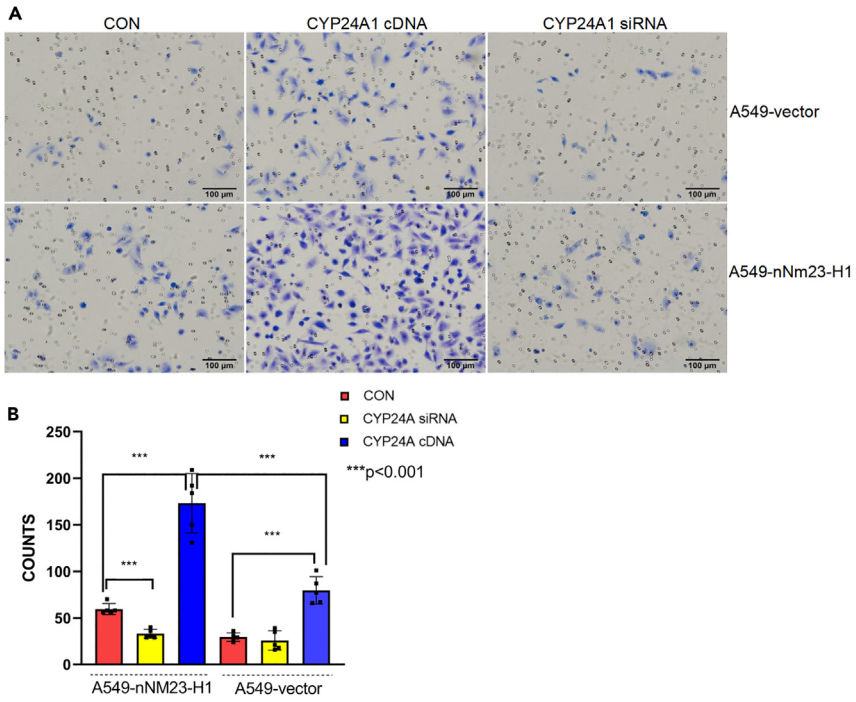

Figure 2. Effect of NME1 nuclear translocation on the migration ability of A549 cells

(A and B) NME1 nuclear translocation enhances the migration ability of A549 cells, while over-expression of CYP24A1 enhances the migration ability of A549-vector cells and A549-nNm23-H1 cells.

Data are the means ± SEM of five experiments. ***$p < 0.001$.

Genes that showed significant differential expression in the *NME1* nuclear translocation and early postoperative metastatic groups were selected as candidates for early validation compared to the control groups. The included genes are *CYP24A1*, *CXCL5*, *CP*, *PON3*, and *POF1B*. Among these genes, *CYP24A1*, which exhibited considerable differential expression and is recognized for its involvement in lung cancer prognosis (Figure 1F), was selected as a focus for additional analysis. In previous studies,[17] *CYP24A1* was identified as an independent prognostic factor in patients with lung adenocarcinoma, with respective 5-year survival rates of 81% and 42% for patients expressing low and high mRNA levels of *CYP24A1*.

Following this, the up-regulation of *CYP24A1* and its downstream protein target β-catenin, which strongly correlates with predictive outcomes in lung cancer, was confirmed in A549-nNm23-H1 using western blotting (Figures 1G and 1H).[18–20] There was no increase in the expression of *CYP24A1* in A549-siNm23-H1 cells where *NME1* had been suppressed, indicating that the up-regulation of *CYP24A1* in A549-nNm23-H1 cells is not caused by the decrease of *NME1* in the cytoplasm after its relocation to the nucleus. Instead, this effect is due to the localization of *NME1* in the nucleus. These results suggest that *NME1* nuclear translocation can regulate the expression of *CYP24A1*.

Nuclear *NME1* enhances the invasive and migratory activity of A549 cells through its ability to regulate the expression of *CYP24A1*

In order to confirm this, the *CYP24A1* gene was deliberately increased in both A549-nNm23-H1 and A549-vector cells. Subsequent transwell tests were performed to evaluate the impact of *CYP24A1* over-expression on the migration and invasion of A549-vector cells. The results showed that *CYP24A1* over-expression increased these activities in A549-vector cells and further enhanced them in A549-nNm23-H1 cells (Figures 2 and 3). When a siRNA construct was used to knock down *CYP24A1* in A549-nNm23-H1 and A549-vector cells, transwell assays demonstrated that the loss of *CYP24A1* was sufficient to reverse the changes in migration and invasion observed in A549-nNm23-H1 cells (Figures 2 and 3). The rescue experiment confirmed that the knockout of *CYP24A1* in A549-nNm23-H1 cells successfully reversed the malignant phenotype associated with *NME1* nuclear translocation.

Nuclear *NME1* up-regulates JUN's transcription activation by binding to it, thereby promoting *CYP24A1* promoter activity and up-regulating its expression

To clarify the mechanisms whereby the nuclear *NME1* controls *CYP24A1* expression, we performed the cleavage under targets and tagmentation (CUT&Tag) assay to assess the DNA-binding profiles of *NME1*. CUT&Tag using antibodies against *NME1* and analysis with deepTools revealed that DNA-binding profiles of *NME1* do not contain *CYP24A1*. The data have been deposited in NCBI-SRA: PRJNA1088718.

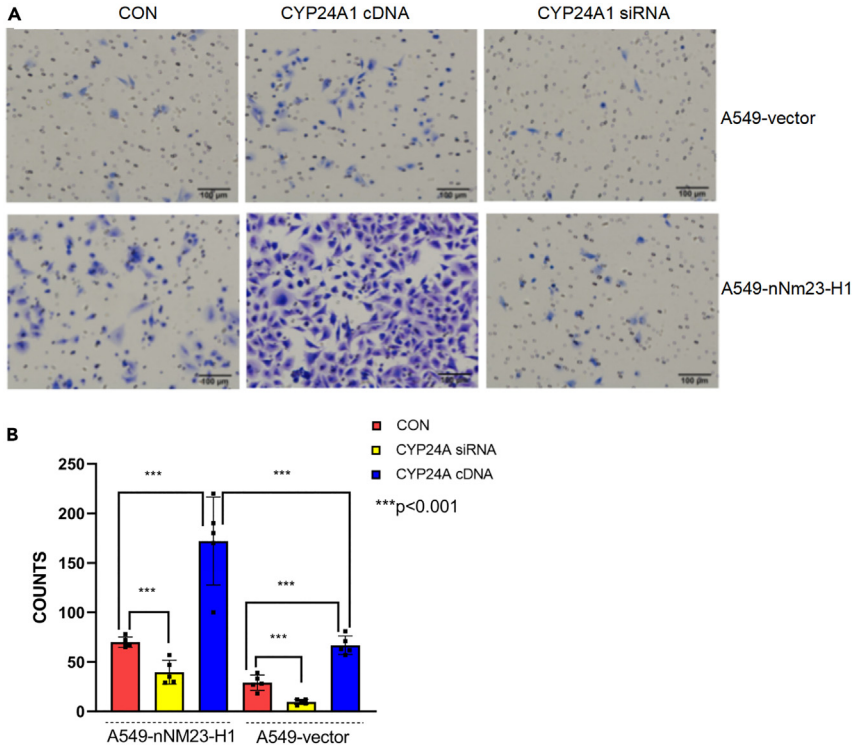

Figure 3. Effect of NME1 nuclear translocation on the invasive ability of A549 cells

(A and B) NME1 nuclear translocation enhances the invasive ability of A549 cells, while over-expression of CYP24A1 enhances the invasive ability of A549-vector cells and A549-nNm23-H1 cells.

Data are the means ± SEM of five experiments. ***$p < 0.001$.

We conduct online predictive analysis to verify whether nuclear *NME1* regulates *CYP24A1* as a transcriptional coactivator (https://jaspar.genereg.net/analysis). Two potential AP-1 binding sites were identified within the *CYP24A1* promoter (relative score ≥0.9), including JUN and C-FOS:JUN binding sites (Figure 4A). These two binding sites were used to design two 5'biotinylated *CYP24A1* promoter DNA probes, two unlabeled DNA probes, and two mutated DNA probes, which were then purified via an HPLC approach. A follow-up super-shift EMSA study verified the enduring attachment of *NME1*, JUN, and the *CYP24A1* promoter sequences, although limited attachment activity was observed between *NME1*, C-FOS, and the *CYP24A1* promoter (Figures 4B and S2A).

To test the functional effects of binding between *NME1*, JUN, and the *CYP24A1* promoters, two dual fluorescent enzyme plasmids encoding the *CYP24A1* promoter with wild-type (WT) or mutated (MUT) C-FOS: JUN binding sites at position −1570 to −1558 (*CYP24A1*-MUTα) and mutated JUN binding sites at position −1176 to −1170 (*CYP24A1*-MUTβ) were constructed (Figure 4C). In the following experiments using dual-luciferase reporter assays, the increased expression of JUN significantly enhanced the luciferase activity of *CYP24A1*-WT in both A549-vector and A549-nNm23-H1 cells. However, it did not impact the activity of *CYP24A1*-MUTβ (Figures 4D and S2B). *CYP24A1* WT luciferase activity in A549-nNm23-H1 cells remained more substantial than in A549 cells, irrespective of whether or not JUN was over-expressed. These results suggested that *CYP24A1* is regulated by JUN and that nuclear *NME1* functions as a transcriptional coactivator to enhance the ability of JUN to activate transcription from the *CYP24A1* promoter. Western blotting also verified that nuclear *NME1* does not regulate JUN phosphorylation via kinase activity (Figure S3).

Nuclear *NME1* expression is positively correlated with the expression of *CYP24A1* and is associated with poor prognosis in lung adenocarcinoma patients

Subsequent retrospective analyses were performed on clinical data obtained from 117 patients undergoing stage I lung adenocarcinoma surgery (Table 1). Immunohistochemistry was then utilized to examine the expression of nuclear *NME1* and *CYP24A1* in tissue sections preserved in formalin-fixed paraffin. 10 samples (8.5%) exhibited clear nuclear *NME1* expression. Those patients exhibiting nuclear *NME1* expression were significantly more likely to experience distant metastasis ($p = 0.001$), and patients with nuclear *NME1* expression have a higher proportion of *CYP24A1* strongly positive expression ($p = 0.049$) than patients without nuclear *NME1* expression. Kaplan-Meier survival analyses indicated that the median disease-free survival (DFS) and disease-specific survival (DSS) of patients with and without nuclear *NME1* expression were 32.82 months vs. un-reached (hazard ratio [HR], 6.202 [95% confidence of interval [CI], 1.26–30.47]; $p = 0$ 0.001) and

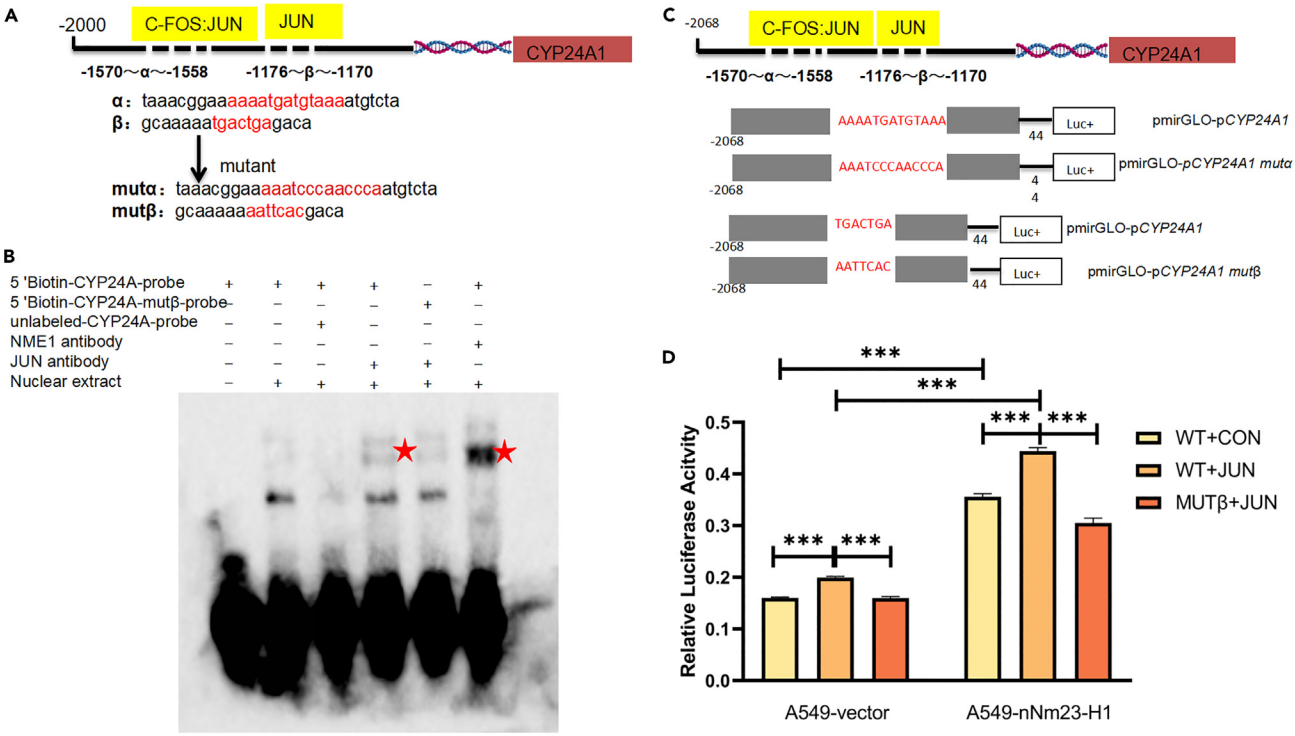

Figure 4. Nuclear NME1 up-regulates the expression of CYP24A1 through binding to JUN

(A) The location of JUN and FOS:JUN target sites in CYP24A1 promoter and the mutation site of CYP24A1 promoter. Construct DNA probes based on these base sequences for super-shift EMSA.

(B) The stable binding of NME1, JUN, and CYP24A1 was validated by super-shift EMSA.

(C) The location of JUN and C-FOS:JUN target sites in CYP24A1 promoter and the mutation site of CYP24A1 promoter.

(D) Dual-luciferase reporter assay analyzed the effect of nuclear NME1 combined with JUN on the activity of CYP24A1 promoter.

Data are the means ± SEM of three experiments. ***$p < 0.001$.

36.55 months vs. un-reached (HR, 11.33 [95% CI, 1.54–83.60]; $p = 0$ 0.001), respectively (Figures 5A and 5B). The mDFS and mDSS were not reached in both high and low *CYP24A1* expression groups, but the difference was significant (HR, 1.80 [95% CI,0.87–3.72]; $p = 0$ 0.049; HR, 3.021 [95% CI,1.04–8.14]; $p = 0$ 0.02) (Figures 5C and 5D).

DISCUSSION

Prior results revealed that radiotherapy can promote *NME1* nuclear translocation,[4] and another study further demonstrated the relocation of *NME1* to the nucleus following exposure to gamma irradiation.[21] The invasion and migration of tumor cells play a crucial role in tumor metastasis. This study confirmed through *in vitro* experiments that A549 cells with *NME1* nuclear translocation have enhanced invasion and migration abilities. Clinical samples also confirmed that early lung adenocarcinoma patients with *NME1* nuclear expression are more prone

Table 1. Correlations between NME1 nuclear expression and distant metastasis, recurrence, and CYP24A1 expression

Characteristic		nNME1	non- nNME1	P
Metastasis, n (%)	Yes	7 (70.0)	22 (20.6)	0.001
	No	3 (30.0)	85 (79.4)	
Metastasis or recurrence, n (%)	Yes	8(80.0)	29 (27.1)	0.001
	No	2 (20.0)	78 (72.9)	
CYP24A1, (%)	High	6 (60.0)	31 (20.0)	0.044
	Low	4 (40.0)	76 (20.0)	

nNME1: NME1 nuclear expression; non-nNME1: without NME1 nuclear expression.

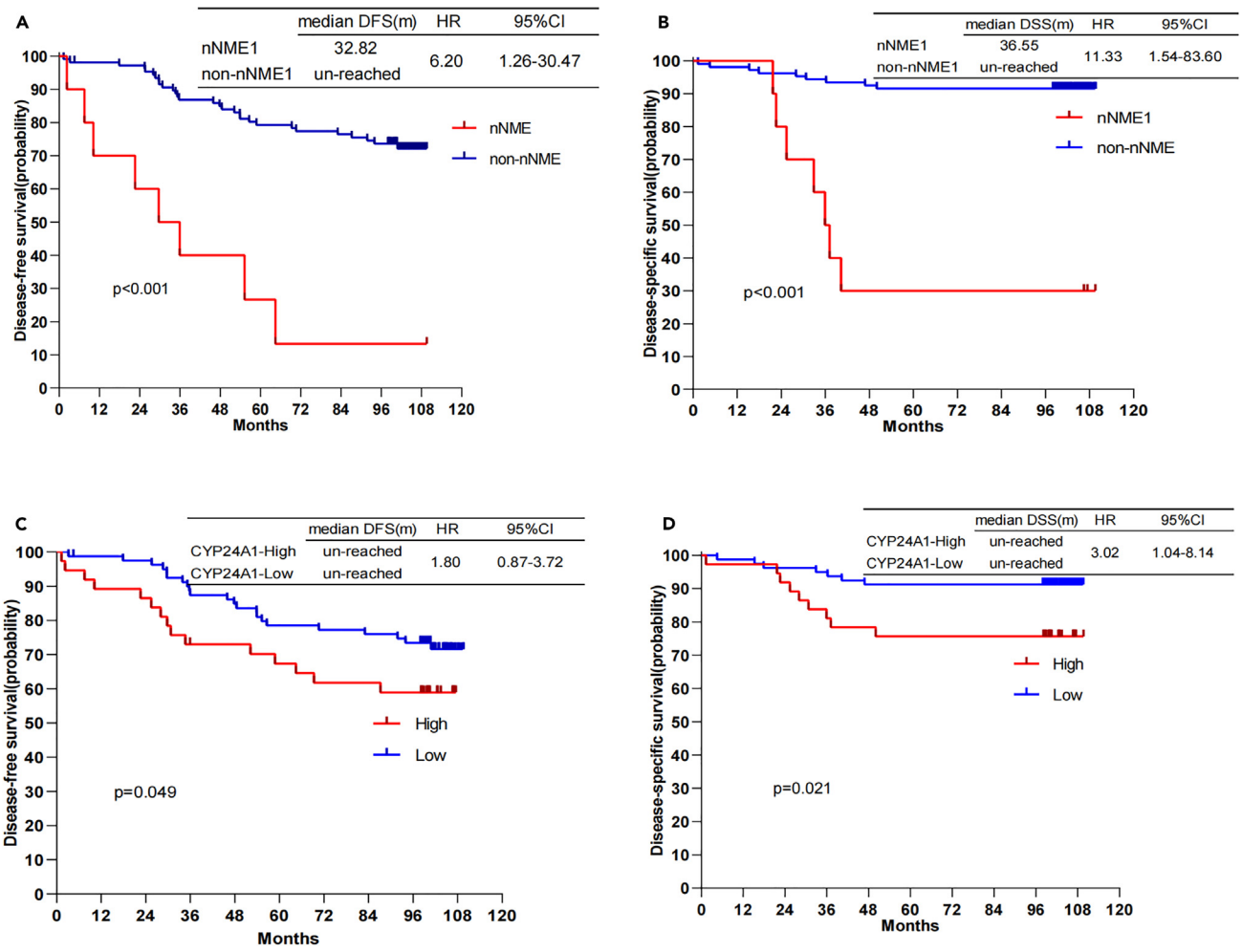

Figure 5. Kaplan-Meier analyses of postoperative lung cancer patients

(A) Disease-free survival by Kaplan-Meier analyses based on whether the patient has nuclear NME1 expression.

(B) Disease-specific survival by Kaplan-Meier analyses based on whether the patient has nuclear NME1 expression.

(C) Disease-free survival by Kaplan-Meier analyses based on the expression level of CYP24A1 in lung cancer cells.

(D) Disease-specific survival by Kaplan-Meier analyses based on the expression level of CYP24A1 in lung cancer cells.

to postoperative distant metastasis and are associated with shorter overall survival. This indicates that lung adenocarcinoma cells with *NME1* nuclear expression have stronger distant metastasis ability and affect the prognosis of early lung adenocarcinoma patients after surgery.

The current findings further illustrated the dual function of *NME1* as both an inhibitor and promoter of metastatic tumor growth. Based on these findings, the movement of *NME1* to the nucleus caused by radiation could be a method via which radiation can enhance the spread of cancer cells to other parts of the body. These results suggest a potential area for further investigation. However, the precise mechanisms whereby *NME1* can modulate invasive and metastatic activity have remained poorly documented. This study presents the initial evidence indicating that the capacity of *NME1* to enhance the invasion and spread of lung tumors can be attributed to its translocation into the cell nucleus and subsequent role as a transcriptional coactivator in tumor cells.

Given that *NME1* is a potential transcription factor,[22–25] we first demonstrated using CUT&Tag that *NME1* cannot bind to the DNA of *CYP24A1* in A549-nNm23-H1 cells, ruling out the possibility of *NME1* acting as a transcription factor to regulate *CYP24A1* expression. In addition, several catalytic functions have been ascribed to cytoplasmic *NME1*.[26–30] In a previous study on repairing DNA damage, we determined that nuclear *NME1* could modulate the phosphorylation of the nuclear checkpoint pathway proteins ATM, p53, and Chk2.[31] Therefore, we also used western blotting to confirm that nuclear *NME1* cannot regulate the phosphorylation of JUN. After excluding the aforementioned two regulatory mechanisms, *NME1* is also capable of regulating a range of target genes through mechanisms that depend on other proteins or transcription factors.[3,23,32–34] We further confirmed by super-shift EMSA and dual-luciferase reporter assays that *NME1*, *CYP24A1*, and JUN

can stably bind and form functional complexes, enhancing the activity of the *CYP24A1* promoter and promoting its expression, confirming that nuclear *NME1* regulates the target gene *CYP24A1* by binding to the transcription factor JUN.

Considering the numerous previous studies that have examined the role of *NME1* in promoting cancer, it is essential to acknowledge the potential influence of viral antigens in this context. However, this process currently lacks systematic or comprehensive information regarding the specific target genes and transcriptional regulatory mechanisms involved. In the present study, a vector containing a nuclear localization signal was employed to cause the translocation of *NME1* protein to the nucleus of A549 cells. This enabled the investigation of the biological consequences of this nuclear localization and the underlying molecular mechanisms. In addition, we verified through western blotting that NME2 did not undergo nuclear translocation in A549-nNm23-H1, indicating that it is indeed *NME1* rather than its highly homologous NME2 in nucleotide and amino acid sequences that up-regulates *CYP24A1* expression, ruling out the influence of NME2 on the research results. Therefore, these findings exhibit a significant level of dependability.

In summary, nuclear *NME1* expression can enhance invasion and migration of A549 cells via the up-regulation of *CYP24A1* through its binding to JUN, thereby influencing prognostic outcomes in patients with lung adenocarcinoma. Based on these findings, further research is necessary to elucidate the multiple functions of *NME1* as both a promoter and inhibitor of cancer malignancy. Furthermore, the nuclear expression of *NME1* holds potential as a predictive tool and therapeutic target for distant metastasis of lung adenocarcinoma in future studies.

Limitations of the study

Our work demonstrates that nuclear *NME1* up-regulates the expression of *CYP24A1* by binding to JUN, enhances the invasion and migration ability of A549 cells, and affects the prognosis of lung adenocarcinoma patients. Nevertheless, we exclusively employed the A549 cell line and intend to incorporate various cell lines for future investigations. Furthermore, further investigations are required to ascertain if nuclear *NME1* has a similar impact on the expression of other target genes by influencing the transcription activation of JUN. Additionally, more research is needed to understand the interaction mechanism between *NME1* and JUN after they bind together.

STAR★METHODS

Detailed methods are provided in the online version of this paper and include the following:

- KEY RESOURCES TABLE
- RESOURCE AVAILABILITY
  - Lead contact
  - Materials availability
  - Data and code availability
- EXPERIMENTAL MODEL AND STUDY PARTICIPANT DETAILS
  - Patient samples and healthy donors
- METHOD DETAILS
  - Immunohistochemical (IHC)
  - Vector construction
  - Cell lines, culture conditions, and transfection
  - Total RNA extraction, library construction, and sequencing
  - Protein extraction and Western blotting analysis
  - Quantitative real-time PCR
  - *CYP24A1* siRNA and JUN siRNA knock-down
  - *CYP24A1* or JUN over-expression assay
  - CCK-8 assay
  - Transwell assay
  - Super-shift EMSA
  - Dual-luciferase reporter assays
  - CUT&Tag
- QUANTIFICATION AND STATISTICAL ANALYSIS

SUPPLEMENTAL INFORMATION

Supplemental information can be found online at https://doi.org/10.1016/j.isci.2024.110286.

ACKNOWLEDGMENTS

This work was supported by the National Natural Science Foundation of China (NSFC, no. 82002443) and the Natural Science Foundation of Chongqing Municipality (cstc2020jcyj-msxmX0233).

AUTHOR CONTRIBUTIONS

X.M. took part in most experiments and writing articles and also is the research manager. L.Y. took part in the majority of experiments and data analysis. K.X. took part in the majority of experiments. P.Y. took part in the western blotting and IHC assay. J.Y. participated in the cell culture experimental design. L.M. and Y.X. designed the experiments and helped write the manuscript.

DECLARATION OF INTERESTS

The authors declare no conflict of interest.

Received: February 22, 2024
Revised: March 26, 2024
Accepted: June 13, 2024
Published: June 15, 2024

REFERENCES

1. Sung, H., Ferlay, J., Siegel, R.L., Laversanne, M., Soerjomataram, I., Jemal, A., and Bray, F. (2021). Global Cancer Statistics 2020: GLOBOCAN Estimates of Incidence and Mortality Worldwide for 36 Cancers in 185 Countries. CA. Cancer J. Clin. *71*, 209–249.
2. Steeg, P.S., Bevilacqua, G., Kopper, L., Thorgeirsson, U.P., Talmadge, J.E., Liotta, L.A., and Sobel, M.E. (1988). Evidence for a novel gene associated with low tumor metastatic potential. J. Natl. Cancer Inst. *80*, 200–204.
3. Subramanian, C., Cotter, M.A., 2nd, and Robertson, E.S. (2001). Epstein-Barr virus nuclear protein EBNA-3C interacts with the human metastatic suppressor Nm23-H1: a molecular link to cancer metastasis. Nat. Med. *7*, 350–355.
4. Zhang, Z.M., Yang, X.Q., Wang, D., Wang, G., Yang, Z.Z., Qing, Y., Yang, Z.X., Li, M.X., and Xiang, D.B. (2011). Nm23-H1 protein binds to APE1 at AP sites and stimulates AP endonuclease activity following ionizing radiation of the human lung cancer A549 cells. Cell Biochem. Biophys. *61*, 561–572.
5. Lodillinsky, C., Fuhrmann, L., Irondelle, M., Pylypenko, O., Li, X.Y., Bonsang-Kitzis, H., Reyal, F., Vacher, S., Calmel, C., De Wever, O., et al. (2021). Metastasis-suppressor *NME1* controls the invasive switch of breast cancer by regulating MT1-MMP surface clearance. Oncogene *40*, 4019–4032.
6. Zhang, S., Nelson, O.D., Price, I.R., Zhu, C., Lu, X., Fernandez, I.R., Weiss, R.S., and Lin, H. (2022). Long-chain fatty acyl coenzyme A inhibits NME1/2 and regulates cancer metastasis. Proc. Natl. Acad. Sci. USA *119*, e2117013119.
7. Khan, I., Gril, B., Hoshino, A., Yang, H.H., Lee, M.P., Difilippantonio, S., Lyden, D.C., and Steeg, P.S. (2022). Metastasis suppressor NME1 in exosomes or liposomes conveys motility and migration inhibition in breast cancer model systems. Clin. Exp. Metastasis *39*, 815–831.
8. Zhang, Y., Zhao, G., Yu, L., Wang, X., Meng, Y., Mao, J., Fu, Z., Yin, Y., Li, J., Wang, X., and Guo, C. (2023). Heat-shock protein 90α protects NME1 against degradation and suppresses metastasis of breast cancer. Br. J. Cancer *129*, 1679–1691.
9. Li, D., Li, W., Tian, C., Pang, Y., Xu, L., Wang, Y., and Xu, X. (2022). Prognostic and clinicopathological significance of nm23-H1 expression in non-small cell lung cancer: A meta-analysis. Medicine (Baltim.) *101*, e30815.
10. Tomita, M., Ayabe, T., Matsuzaki, Y., and Onitsuka, T. (2001). Expression of nm23-H1 gene product in mediastinal lymph nodes from lung cancer patients. Eur. J. Cardio. Thorac. Surg. *19*, 904–907.
11. Gazzeri, S., Brambilla, E., Negoescu, A., Thoraval, D., Veron, M., Moro, D., and Brambilla, C. (1996). over-expression of nucleoside diphosphate/kinase A/nm23-H1 protein in human lung tumors: association with tumor progression in squamous carcinoma. Lab. Invest. *74*, 158–167.
12. Tan, C.Y., and Chang, C.L. (2018). NDPKA is not just a metastasis suppressor - be aware of its metastasis-promoting role in neuroblastoma. Lab. Invest. *98*, 219–227.
13. Niitsu, N., Nakamine, H., Okamoto, M., Akamatsu, H., Honma, Y., Higashihara, M., Okabe-Kado, J., and Hirano, M.; Adult Lymphoma Treatment Study Group, ALTSG (2003). Expression of nm23-H1 is associated with poor prognosis in peripheral T-cell lymphoma. Br. J. Haematol. *123*, 621–630.
14. Kim, S.H., Lee, S.Y., Park, H.R., Sung, J.M., Park, A.R., Kang, S., Kim, B.G., Choi, Y.P., Kim, Y.B., and Cho, N.H. (2011). Nuclear localization of Nm23-H1 in head and neck squamous cell carcinoma is associated with radiation resistance. Cancer *117*, 1864–1873.
15. Ismail, N.I., Kaur, G., Hashim, H., and Hassan, M.S. (2008). Nuclear localization and intensity of staining of nm23 protein is useful marker for breast cancer progression. Cancer Cell Int. *8*, 6.
16. Sheng, Y., Xiong, Y., Xu, M., Kuang, X., Wang, D., and Yang, X. (2017). Effect of Nm23-H1 Nuclear Localization on Proliferation of Human Lung Adenocarcinoma Cell Line A549. Zhongguo Fei Ai Za Zhi *20*, 226–232.
17. Chen, G., Kim, S.H., King, A.N., Zhao, L., Simpson, R.U., Christensen, P.J., Wang, Z., Thomas, D.G., Giordano, T.J., Lin, L., et al. (2011). CYP24A1 is an independent prognostic marker of survival in patients with lung adenocarcinoma. Clin. Cancer Res. *17*, 817–826.
18. Yin, N., Liu, Y., Khoor, A., Wang, X., Thompson, E.A., Leitges, M., Justilien, V., Weems, C., Murray, N.R., and Fields, A.P. (2019). Protein Kinase Cι and Wnt/β-Catenin Signaling: Alternative Pathways to Kras/Trp53-Driven Lung Adenocarcinoma. Cancer Cell *36*, 156–167.e7.
19. He, Y., Jiang, X., Duan, L., Xiong, Q., Yuan, Y., Liu, P., Jiang, L., Shen, Q., Zhao, S., Yang, C., and Chen, Y. (2021). LncRNA PKMYT1AR promotes cancer stem cell maintenance in non-small cell lung cancer via activating Wnt signaling pathway. Mol. Cancer *20*, 156.
20. Pan, J., Fang, S., Tian, H., Zhou, C., Zhao, X., Tian, H., He, J., Shen, W., Meng, X., Jin, X., and Gong, Z. (2020). lncRNA JPX/miR-33a-5p/Twist1 axis regulates tumorigenesis and metastasis of lung cancer by activating Wnt/β-catenin signaling. Mol. Cancer *19*, 9.
21. Radić, M., Šoštar, M., Weber, I., Ćetković, H., Slade, N., and Herak Bosnar, M. (2020). The Subcellular Localization and Oligomerization Preferences of NME1/NME2 upon Radiation-Induced DNA Damage. Int. J. Mol. Sci. *21*, 2363.
22. Ma, D., Xing, Z., Liu, B., Pedigo, N.G., Zimmer, S.G., Bai, Z., Postel, E.H., and Kaetzel, D.M. (2002). NM23-H1 and NM23-H2 repress transcriptional activities of nuclease-hypersensitive elements in the platelet-derived growth factor-A promoter. J. Biol. Chem. *277*, 1560–1567.
23. Curtis, C.D., Likhite, V.S., McLeod, I.X., Yates, J.R., and Nardulli, A.M. (2007). Interaction of the tumor metastasis suppressor nonmetastatic protein 23 homologue H1 and estrogen receptor alpha alters estrogen-responsive gene expression. Cancer Res. *67*, 10600–10607.
24. Cervoni, L., Egistelli, L., Eufemi, M., Scotto d'Abusco, A., Altieri, F., Lascu, I., Turano, C., and Giartosio, A. (2006). DNA sequences acting as binding sites for NM23/NDPK proteins in melanoma M14 cells. J. Cell. Biochem. *98*, 421–428.
25. Xie, M., Zhang, L., Han, L., Huang, L., Huang, Y., Yang, M., and Zhang, N. (2023). The ASH1L-AS1-ASH1L axis controls NME1-mediated activation of the RAS signaling in gastric cancer. Oncogene *42*, 3435–3445.
26. Moréra, S., Lascu, I., Dumas, C., LeBras, G., Briozzo, P., Véron, M., and Janin, J. (1994). Adenosine 5'-diphosphate binding and the active site of nucleoside diphosphate kinase. Biochemistry *33*, 459–467.
27. Adam, K., Ning, J., Reina, J., and Hunter, T. (2020). NME/NM23/NDPK and Histidine Phosphorylation. Int. J. Mol. Sci. *21*, 5848.
28. Lecroisey, A., Lascu, I., Bominaar, A., Véron, M., and Delepierre, M. (1995). Phosphorylation mechanism of nucleoside diphosphate kinase: 31P-nuclear magnetic resonance studies. Biochemistry *34*, 12445–12450.
29. Wagner, P.D., and Vu, N.D. (2000). Phosphorylation of geranyl and farnesyl pyrophosphates by Nm23

proteins/nucleoside diphosphate kinases. J. Biol. Chem. *275*, 35570–35576.

30. Lapek, J.D., Jr., Tombline, G., and Friedman, A.E. (2011). Mass spectrometry detection of histidine phosphorylation on NM23-H1. J. Proteome Res. *10*, 751–755.
31. Sheng, Y., Xu, M., Li, C., Xiong, Y., Yang, Y., Kuang, X., Wang, D., and Yang, X. (2018). Nm23-H1 is involved in the repair of ionizing radiation-induced DNA double-strand breaks in the A549 lung cancer cell line. BMC Cancer *18*, 710.
32. Qin, Z., Dai, L., Toole, B., Robertson, E., and Parsons, C. (2011). Regulation of Nm23-H1 and cell invasiveness by Kaposi's sarcoma-associated herpesvirus. J. Virol. *85*, 3596–3606.
33. Mileo, A.M., Piombino, E., Severino, A., Tritarelli, A., Paggi, M.G., and Lombardi, D. (2006). Multiple interference of the human papillomavirus-16 E7 oncoprotein with the functional role of the metastasis suppressor Nm23-H1 protein. J. Bioenerg. Biomembr. *38*, 215–225.
34. Kuppers, D.A., Lan, K., Knight, J.S., and Robertson, E.S. (2005). Regulation of matrix metalloproteinase 9 expression by Epstein-Barr virus nuclear antigen 3C and the suppressor of metastasis Nm23-H1. J. Virol. *79*, 9714–9724.

STAR★METHODS

KEY RESOURCES TABLE

REAGENT or RESOURCE	SOURCE	IDENTIFIER
Antibodies		
c-Fos	Abcam	RRID: AB_2891049
c-Jun	Abcam	RRID: AB_726900
p-c-Jun	Abcam	RRID: AB_726902
NME1	Abcam	RRID: AB_10972661
CYP24A1	Proteintech Group	RRID: AB_10792804
IGg	CST	RRID: AB_10694704
c-Jun	CST	RRID: AB_2130165
Biological samples		
Human non-small cell lung cancer tissue	Daping Hospital of Army Medical University	N/A
Chemicals, peptides, and recombinant proteins		
Kanamycin	Solarbio	K1030
Double luciferase plasmid c-Fos	Sangon Biotech	N/A
Double luciferase plasmid c-Jun	Sangon Biotech	N/A
Fetal Bovine Serum	VivaCell	C04001
PAGETM 4-20%	ACE	ET15420LGel
Pancreatic enzyme	Boster Biological Technology	PYG0015
Luria-Bertani	Beijing Solarbio Science & Technology	L1010
Filter paper	Bio-Rad,Thermo,Nikon,Buchi	1703965
Pancreatic enzyme	VivaCell	C3530-0100
Fetal Bovine Serum	Procell Life Science&Technology	164210-50
Protein A	CST	73778s
Critical commercial assays		
EMSA Assay Kit	Thermo Fisher Scientific	89880
CUT&Tag Assay Kit	Nanjing Vazyme Biotech	TD903
Cell Counting Kit-8	Baoguang Biotechnology	BG0025
Dual Luciferase Assay Kit	Promega	E1910
Cell lines		
Human A549	ATCC	CL-0016
Oligonucleotides		
hCYP24A1-1567-F-primer:UUACGCC GAGUGUACCAUUUATT	Sangon Biotech	This paper
hCYP24A1-1567-R-primer:UAAAUGG UACACUCGGCGUAATT	Sangon Biotech	This paper
hCYP24A1-699-F-primer:CGCAUGAA GUUGGGUUCCUUUTT	Sangon Biotech	This paper
hCYP24A1-699-R-primer:AAAGGAACC CAACUUCAUGCGTT	Sangon Biotech	This paper
hCYP24A1-1302-F-primer:GCAGAUUU CCUUUGUGACAUUTT	Sangon Biotech	This paper
hCYP24A1-1302-R-primer:AAUGUCACA AAGGAAAUCUGCTT	Sangon Biotech	This paper

(*Continued on next page*)

Continued

REAGENT or RESOURCE	SOURCE	IDENTIFIER
hc-Jun-1-1046-F-primer:CUAAAGAA AGUCAUCCAGAAATT	Sangon Biotech	This paper
hc-Jun-1-1046-R-primer:UUUCUGGAU GACUUUCUUUAGTT	Sangon Biotech	This paper
hc-Jun-1-1931-F-primer:UGGGUGC CAACUCAUGCUAACTT	Sangon Biotech	This paper
hc-Jun-1-1931-R-primer:GUUAGCA UGAGUUGGCACCCATT	Sangon Biotech	This paper
hc-Jun-1-1211-F-primer:CCUGAUAAU CCAGUCCAGCAATT	Sangon Biotech	This paper
hc-Jun-1-1211-R-primer:UUGCUGGAC UGGAUUAUCAGGTT	Sangon Biotech	This paper
GAPDH-F-primer:GUAUGACAA CAGCCUCAAGTT	Sangon Biotech	This paper
GAPDH-R-primer:CUUGAGGCUGU UGUCAUACTT	Sangon Biotech	This paper
FAM NC-F-primer:UUC UCC GAA CGU GUC ACG UTT	Sangon Biotech	This paper
FAM NC-R-primer:ACG UGA CAC GUU CGG AGA ATT	Sangon Biotech	This paper
NC-F-primer:UUC UCC GAA CGU GUC ACG UTT	Sangon Biotech	This paper
NC-R-primer:ACG UGA CAC GUU CGG AGA ATT	Sangon Biotech	This paper
Recombinant DNA		
pmirGLO-CYP24A1-promoter	Sangon Biotech	This paper
pmirGLO-CYP24A1-promoter mutβ	Sangon Biotech	This paper
pmirGLO-CYP24A1-promoter mutα	Sangon Biotech	This paper
pLentis-CMV-NME1-IRES2-PURO	Sangon Biotech	N/A
c-Jun cDNA Plasmid (4685-1)-P1:TCCGCT CGAGATGACTGCAAAGATGGAAACG	Shanghai Genechem	CMV-MCS-EGFP-SV40-Neomycin
c-Jun cDNA Plasmid (4685-1)-P2:ATCGGG ATCCCGAAATGTTTGCAACTGCTGCG	Shanghai Genechem	CMV-MCS-EGFP-SV40-Neomycin
CYP24A1 cDNA Plasmid (63528-22)-p1:TACCG GACTCAGATCTCGAGCGCCACCAT GAGCTCCCCCATCAGCAAG	Shanghai Genechem	CMV-MCS-EGFP-SV40-Neomycin
CYP24A1 cDNA Plasmid (63528-22)-p2:GATCCCGGGCCCGCGGTACC GTTCGCTGGCAAAACGCGATGGGGAG	Shanghai Genechem	CMV-MCS-EGFP-SV40-Neomycin
Software and algorithms		
SPSS Statistics version 19.0	IBM	version 23.0
Graph-Pad Prism	GraphPad	version 8.0.2
R software	R	version 4.0.2
Image J	N/A	version 1.54d
Image Lab	N/A	version 6.0
Trimmomatic	N/A	version 0.39
FastQC	N/A	version 0.11.9

(*Continued on next page*)

Continued

REAGENT or RESOURCE	SOURCE	IDENTIFIER
FeatureCounts	N/A	version 2.0.1
Bowtie2	N/A	version 2.4.4
Samtools	N/A	version 1.13
Picard	N/A	N/A
MACS2	N/A	version 2.1.4
Deeptools	N/A	version 3.5.1
IGV	N/A	N/A
Homer	N/A	N/A

RESOURCE AVAILABILITY

Lead contact

Further information and requests for resources and reagents should be directed to and will be fulfilled by the lead contact, Mingfang Xu (xusiyi023@126.com).

Materials availability

This study did not generate new unique reagents.

Data and code availability

- CUT&TAG data have been deposited at [datatype-specific repository] and are publicly available as of the date of publication. The data have been deposited in NCBI-SRA: PRJNA1088718.
- This paper does not report original code.
- Any additional information required to reanalyze the data reported in this paper is available from the lead contact upon request.

EXPERIMENTAL MODEL AND STUDY PARTICIPANT DETAILS

Patient samples and healthy donors

Human subjects

All subjects were from Daping hospital. Subjects with postoperative pathological diagnosis of lung adenocarcinoma who underwent radical lung cancer surgery in our hospital, from January 2015 to January 2016, were included in this study. Inclusion criteria: 1)R0 re section. 2) The postoperative pathological diagnosis was lung adenocarcinoma. 3) The postoperative pathological staging is stage I(AJCC 8th). 4) Patients who agree to be followed up. Exclusion criteria: Patients without sufficient pathological specimens. Finally, a total of 117 adult subjects were included in this study. All subjects underwent medical history records and postoperative immunohistochemical testing of lung cancer tissue. Disease-free survival(DFS) is defined as the time from the date of surgery to recurrence, metastasis or the last follow-up.Disease specific survival(DSS) is defined as the time interval from the date of surgery to lung cancer death or the last follow-up. All plans were implemented in accordance with the 1975 Helsinki Declaration and approved by the Ethics Committee of Daping Hospital under the approval numbers 2020–120. The requirement for obtaining informed consent was waived because of the study's retrospective design, and all patient data has been anonymized. All patients are Han Chinese, including 70 males and 47 females, with ages ranging from 41 to 78 years old.

No animal model was used in this study.

METHOD DETAILS

Immunohistochemical (IHC)

Lung cancer tissues were fixed in a 4% paraformaldehyde solution for 24 h, embedded in paraffin. The paraffin section of the patient's tumor tissue is made into a tissue chip, and the preparation process is as follows: first, a puncture needle is used to drill holes on the recipient wax block, and then a tissue wax core is taken at the sampling site of the donor wax block using a sampling needle, and the tissue wax core is pushed into the recipient wax core. By repeatedly arranging the tissue wax cores in an orderly manner and moving them into the recipient wax block, a tissue chip wax block is produced; then, slice the above-mentioned tissue chip wax block with a thickness of 3–4 μm for IHC staining. IHC staining was performed on tissue chips using *NME1* antibody(Santa Cruz Biotechnology, sc-514515,dilution 1:3000,USA) and *CYP24A1* antibody (proteintech, 21582-1-AP,dilution 1:3000,USA) to observe the expression of *NME1* and *CYP24A1*. IHC results were observed and captured with a light microscope(OLYMPUS BX53, Olympus, Tokyo, Japan). According to whether *NME1* is expressed in the nucleus, it is divided into n*NME1* and non-n*NME1*. According to the expression of *CYP24A1*, it is divided into high expression and low expression."+++" is defined as high expression, and negative to "++" is defined as low expression.

Vector construction

As reported in our previous research,[31] the pLentis-CMV-*NME1*-IRES2-PURO lentivirus vector over expressed *NME1* was constructed with nuclear located sequence(NLS), and stably transfected into A549 cells for introducing *NME1* into nucleus(A549-nNm23-H1). The pLentis-CMV-PURO empty lentivirus vector containing only nuclear localization sequences(NLS) was used as a control(A549-vector). We also constructed a vector that conditional suppressed *NME1* with Dox-regulated vector system. *NME1*-shRNA was introduced into Lentis-BiD-tetO-H1-SFFV-GFP vector carrying the green fluorescent protein(GFP) reporter gene driven by the SFFV promoter and a tetracycline operator, and stably transfected into A549 cells for suppressing *NME1*(A549-shNm23-H1).

The *CYP24A1* and JUN plasmids were obtained from Genechem(Shanghai, China). Small interfering RNAs(siRNAs) targeting *CYP24A1* and JUN were directly synthesized(Sangon Biotech, China). Transfection of plasmids or siRNAs was conducted using HiperFect Transfection Reagent(QIAGEN,166026259,Germany). Cells were collected for further experiments two days after transfection. Sequences are listed in the key resources table.

Cell lines, culture conditions, and transfection

Human A549-vector and A549-nNm23-H1 cells were cultured in DMEM/H(Pricella,PM150210,China) with 10% fetal bovine serum(FBS, Pricella,164210-50,China),and 1% penicillin-streptomycin(Pricella,PB180120,China), in a 5%CO2 atmosphere at 37°C. Cell lines were tested for mycoplasma contamination and validated by short tandem repeat (STR) polymorphism analysis performed by the Life code genomic technologies.

Total RNA extraction, library construction, and sequencing

RNA sequencing was performed on A549-nNm23-H1 cells, A549-shNm23-H1 cells, and A549-vector cells, using three biological replicates per group. At the same time, RNA sequencing was performed on lung adenocarcinoma specimens from patients who rapidly metastasized within 1 year after surgery or did not recur within 3 years of follow-up, using three biological replicates per group.

Total RNA was isolated using the Trizol method according to manufacturer's instructions. RNA quality was measured using the Simply Total RNA Extraction Kit(BioFlux,BSC52M1,USA). cDNA libraries for each sample were constructed as reported previously. Libraries were sequenced on BGIseq500 platform(BGI-Shenzhen, China), using 150 bp paired-end reads aimed at 30 million reads per sample. The raw sequencing data was filtered with Trimmomatic(v0.39) by removing reads containing sequencing adapter and reads with low-quality base. The clean reads were mapped to the reference genome(mm10) using Hisat2(v2.4.4). Quantification of gene expression was calculated using FeatureCounts(v2.0.1), converted to transcripts per million(TPM) using the R software. We conducted a differential gene expression analysis comparing early postoperative metastasis versus non-early postoperative metastasis, and A549-nNm23-H1 cells versus A549-vector. Subsequently, differential expression analysis between groups was conducted using the R/DESeq2(1.3.40) with adjust p value <0.05 and log2FC > 2.

Protein extraction and Western blotting analysis

Proteins were extracted with T-PER Tissue Protein Extraction Reagent(Thermo scientfic,XA339903,USA)containing protease and phosphatase inhibitors(TargetMol 14K19B46 USA) and were quantified using Rapid BCA Protein Assay Kit(BOSTER,14K19B46 USA) according to the manufacturer's instructions. Western blotting analysis was performed as previously described. Briefly, 40μg lysate was loaded onto SDS-PAGE gels, blotted onto polyvinylidene difluoride(PVDF) membranes(BIO-RAD,1620177,USA), and incubated with antibodies. The primary antibodies used in this work including anti-NME1(Santa Cruz Biotechnology,sc-514515,dilution 1:3000), anti-CYP24A1(proteintech, 21582-1-AP, dilution 1:500), anti-β-Catenin(Abcam,ab32572, dilution 1:5000), anti-JUN(CST, 9165S, dilution 1:1000), anti-p-JUN(Abcam, ab32385, dilution 1:1000).

Quantitative real-time PCR

TRIzol method(Thermo Fisher) was used to extract total RNA from tissues and cells according to the manufacturer's instructions. Briefly, 1μg RNA was converted into cDNA using High-Capacity cDNA Reverse Transcription Kit(Thermo Fisher), and QPCR was performed with a CFX96 Real-Time system(BIO-RAD,USA) using C1000 Thermal Cyclear(BIO-RAD,USA) according to the manufacturer's instructions. Tbp or18s was used as the endogenous control.

CYP24A1 siRNA and JUN siRNA knock-down

SiRNA-mediated knock-down of CYP24A1 and JUN was conducted in A549-nNm23-H1 cells and A549-vector cell lines. HiperFect Transfection Reagent(QIAGEN,1029975,Germany) was used as transfection reagent according to the instruction manual and the transfection was carried out in six replicates. On the next day, we harvested the cells, extracted RNA, performed reverse transcription, and measured the expression of CYP24A1 and JUN by RT-qPCR. GAPDH was used as housekeeping gene.

CYP24A1 or JUN over-expression assay

CYP24A1 or JUN was over-expressed in A549-nNm23-H1 cells and A549-vector cells using a CYP24A1 or JUN expressing plasmid. In the first experiment, 125,000 A549-nNm23-H1 cells or A549-vector cells were transfected with 25ng, 50ng, 75ng, or 100ng of a CYP24A1 or JUN expression vector under a CMV promoter(pLV[Exp]-CMV>hCYP24A1 or JUN [GenBank: NM_001273.5], VectorBuilder). In a second

experiment, 450,000 A549-nNm23-H1 cells or A549-vector cells were transfected with 2.5ug of the CYP24A1 or JUN expression vector, respectively. ViaFect Transfection Reagent(QIAGEN,E498A,Germany) was used as transfection reagent according to the instruction manual and the transfection was carried out in three to four replicates. At the next day, the cells were harvested and RNA was extracted and reverse transcribed to perform RT-qPCR. The expression of CYP24A1 and JUN was measured. GAPDH was used as housekeeping gene.

CCK-8 assay

Inoculate cells into 96 well plates and incubate for 48 h. Then, 10 μL CCK-8 reagent(BaoGuang, BG0025, China) was added to each well for further cultivation for 2 h. Test the absorbance at 450nm using a Molecular Devices(USA) reader.

Transwell assay

The transwell chamber coating Matrigel(Corning) was applied or not for transwell invasion assay and the migration assay. Place cells resuspended in 200 μL serum free medium into the upper chamber and 400 μL complete medium into the lower chamber. After 24 h, the cells transferred into the lower chamber were fixed and stained with methanol and crystal violet. Inverted microscope(Olympus, Japan) is used to observe and count their quantity.

Super-shift EMSA

To further confirm that binding of JUN, CYP24A1 and NME1, we designed probes from the region of the promoter bearing CYP24A1 binding site(heterodimer c-Fos: JUN binding site aaaaaatgatgtaaa and homodimer JUN binding site tgactga), and constructed 5 'Biotin labeled CYP24A1 RNA probes and mutation probes, and purified by HPLC technology. Super-Shift EMSA was performed using the Nuclear and Cytoplasmic Protein Exrtraction Kit(Beyotime, 080321211117,China) according to manufacturer's instructions. NME1,JUN/c-Fos specific antibody and CYP24A1 probes were included in the binding reactions, incubated on ice or at room temperature and resolved by PAGE in a 7.5% native gel to assess specific binding of the transcription factor on CYP24A1 promoter.The labeled probes were incubated with 2–4 μg of Sp2/O or primary murine B cell nuclear extract prepared using the NE-PER kit in presence of 10% Glycerol, 1ug/ul Poly dI:dC and 1×binding buffer supplied with the kit, for 20 min at room temperature. The binding reactions were resolved on 7.5% native PAGE, transferred to a Nylon transfer membrane(HyBond N+)(Amersham, Piscataway, NJ). The shifts were detected using chemiluminescence.

Dual-luciferase reporter assays

To evaluate promoter activity in A549-nNm23-H1 and A549-vector cells, the CYP24A1 promoter sequence(−2068/ +44) containing AP1 binding sites was loaded into the pmirGlo vector to construct the dual-luciferase reporter plasmid(pmirGLO-CYP24A1-promoter, Sangon Biotech, Shanghai, China). The mutant dual-luciferase reporter plasmid were constructed by mutate -1176∼-1170(predicted JUN binding site, TGACTGA to AATTCAC, pmirGLO-CYP24A1-promoter mutβ, Sangon Biotech, Shanghai, China)or -1570∼-1558(predicted cFos:JUN binding site, AAAATGATGTAAA to AAATCCCAACCCA,pmirGLO-CYP24A1-promoter mutα, Sangon Biotech, Shanghai, China)as a control.

A549-nNm23-H1 cells and A549-vector were cultured in 24-well plates and co-transfected with JUN plasmid or cFos:JUN plasmid, dual-luciferase reporter plasmid according to the manufacturer's instructions. After 48 h, cells were harvested and measured using the Dual-luciferase reporter assay system(Promega) according to the manufacturer's instructions. Luciferase activity was normalized to Renilla luciferase activity(control reporter).

CUT&Tag

CUT&Tag analysis was performed as described in a previous study. The CUT&Tag assay was performed using a Hyperactive® Universal CUT&Tag Assay Kit for Illumina(Vazyme Biotech Co.,Ltd) according to the manufacturer's instructions. Briefly, cells were collected at room temperature and counted. Then, the cells required for the experiment were taken in 1.5 mL EP tubes and centrifuged at 600 g for 5 min at low speed at room temperature, and the supernatant was discarded. Add 100ul of pre-cooled NE buffer to each sample, re-suspend the cells by blowing with a pipette gun and incubate on ice for 10min.Then centrifuge at low speed and discard the supernatant. Add 16% formaldehyde to 0.1% and incubate for 2 min, then add 15ul of glycine and leave for 5 min.Then centrifuge at low speed and discard the supernatant.Re-suspend nuclei with 100ul wash buffer.Then add 5ul proteinase K, 100ul buffer L/B, incubate at 60°C for 60 min, during the period of inversion mixing 2–3 times, then add 20ul DNA Extract Beads, vortex well and mix, incubate at room temperature for 5 min.After that, start the ConA Beads treatment, take an octuple tube, add 100ul binding buffer to each sample, add 10ul of well-mixed ConA Beads to each sample, to the magnetic rack, after the solution is clarified, discard the supernatant.Remove the 8-link tubes from the magnetic rack, add 100ul binding buffer, blow to mix, place on the magnetic rack, wait until the solution is clarified and discard the supernatant, add 10ul binding buffer to re-suspend the ConA Beads.The treated cells were transferred to 8-connected tubes with activated ConA Beads, mixed upside down and incubated at room temperature for 10 min, during which they were turned up and down twice.The reaction solution was collected by instantaneous centrifugation, the 8-coupled tubes were placed on a magnetic rack and the supernatant was discarded after the solution was clarified.For each sample, 50ul of pre-cooled Antibody Buffer was added to re-suspend the cell-magnetic bead mixture, antibodies were added, and transient centrifugation was performed overnight at 4°C.The reaction solution was collected by instantaneous centrifugation, and the 8 tubes were placed on a magnetic rack. After the solution was clarified, the supernatant was discarded, the secondary antibody was added, and the solution was mixed thoroughly and incubated for 30 min at room temperature.The reaction solution was collected instantly and

placed on a magnetic rack, the solution was clarified and the supernatant discarded, 200ul of Dig-wash Buffer was added, mixed and repeated 5 times.The reaction solution was collected by transient centrifugation, placed on a magnetic rack, and when the solution was clarified, the supernatant was discarded, and 100ul of diluted pA/G-Tnp transposon was added, mixed thoroughly, and incubated for 1h at room temperature.Centrifuge instantly, place on a magnetic rack, wait until the solution is clarified, discard the supernatant, add 200ul Dig Buffer, mix well and repeat the above steps 3 times.Instantaneous centrifugation, collect the reaction solution, place it on a magnetic rack, wait until the solution is clarified, discard the supernatant, add 50ul of TTBL solution, mix it well and place it in a PCR instrument at 37°C, incubate for 60min.-Add 5ul proteinase K, 100ul buffer L/B and 20ul DNA Extract Beads to the fragmented DNA fragments, vortex and mix thoroughly, and incubate at 55°C for 10min, during which the mixing was inverted twice.Centrifuge instantly, place on a magnetic rack and let stand for 2–3 min, carefully removing the supernatant.Add 200ul buffer WA, vortex thoroughly, centrifuge instantly to collect the reaction solution, let it stand for 2min, discard the supernatant and repeat the above steps once.Dry at room temperature for 5–10 min, add 22ul of sterilized purified water, mix well and elute for 5 min, during which time gently shake 2–3 times.The PCR instrument was then used to amplify the library.Pipette 100ul VAHTS DNA clean beads into the above PCR product, vortex and oscillate, incubate for 5 min, then place on a magnetic rack and remove the supernatant when the solution is clarified.Keeping the PCR tube on the magnetic rack, rinse the magnetic beads by adding 200ul of 80% ethanol, incubate at room temperature for 30 s, carefully remove the supernatant and repeat the above steps once.Open the lid and dry for 3–5 min, sterilized and eluted with ultrapure water, then store in a −20° refrigerator.Finally, the processed samples were sequenced using a Novaseq 6000 instrument. 1 × 105 cells were washed with 1 mL of wash buffer(20mM HEPES pH 7.5, 150mM NaCl, 0.5mM Spermidine(Sigma-Aldrich), 1× Protease inhibitor cocktail(Roche)) and centrifuged at 1,600 r.p.m. for 5 min at room temperature. Cell pellets were resuspended with 1 mL of wash buffer. Concanavalin A-coated magnetic beads(Bangs Laboratories) were washed twice with binding buffer(20mM HEPES pH 7.5, 10mM KCl, 1mM MnCl2, 1mM CaCl2). Next, 10μL of activated beads were added and incubated at room temperature for 15 min. Bead-bound cells were resuspended in 50μL of antibody buffer(20mM HEPES pH 7.5, 150mM NaCl, 0.5mM Spermidine, 0.05% Digitonin(Sigma-Aldrich), 2mM EDTA, 0.1% BSA, 1× Protease inhibitor cocktail). Then, 1μg of primary antibody(mouse monoclonal anti-CHD4 antibody(3F2/4, abcam) or normal mouse IgG(sc-2025, Santa Cruz)) was added and incubated overnight at 4°C with slow rotation. The primary antibody was removed using a magnet stand. Secondary antibody(1 μg)(rabbit anti-mouse IgG H&L(ab6709, abcam)) was diluted in 50μL of Dig-wash buffer(20mM HEPES pH 7.5, 150 mM NaCl, 0.5mM Spermidine, 0.05% Digitonin, 1× Protease inhibitor cocktail) and cells were incubated at room temperature for 1 h. Cells were washed three times with Dig-wash buffer to remove unbound antibodies. The Hyperactive pA-Tn5 Transposase adapter complex(TTE mix, 4 μM, Vazyme) was diluted 1:100 in 100μL of Dig-300 buffer(20mM HEPES pH 7.5, 300mM NaCl, 0.5mM Spermidine, 0.01% Digitonin, 1× Protease inhibitor cocktail). Cells were incubated with 0.04 μM TTE mix at room temperature for 1 h. Cells were washed three times with Dig-300 buffer to remove unbound TTE mix. Cells were then resuspended in 300μL of tagmentation buffer(10 mM MgCl2 in Dig-300 buffer) and incubated at 37°C for 1 h. To terminate tagmentation, 10μL of 0.5 M EDTA, 3μL of 10% SDS and 5μL of 10mg mL−1 Proteinase K were added to 300μL of sample and incubated at 50°C for 1 h. DNA was purified using phenol-chloroform-isoamyl alcohol extraction and ethanol precipitation as well as RNase A treatment. The data have been deposited in NCBI-SRA: PRJNA1088718.

QUANTIFICATION AND STATISTICAL ANALYSIS

All experiments repeat at least three times. Image J software is used to measure the expression of target proteins in Western blotting or IHC. Data were shown as mean ± standard deviation. Students' t test was used in Western blotting, IHC and transwell assay. Categorical data were compared using Chi-squared tests. SPSS 23.0 and GraphPad Prism v8.0.2 were used for analyses and figure construction. Statistical significance was defined as $*p < 0.05$, $**p < 0.01$, $***p < 0.001$.